npj | parkinson's disease

Article

Published in partnership with the Parkinson's Foundation

https://doi.org/10.1038/s41531-025-01075-z

Oligomeric alpha-synuclein causes early synaptic dysfunction of the corticostriatal pathway associated with non-motor symptoms

Check for updates

Laura Bellingacci[1,12], Miriam Sciaccaluga[1,2,11,12], Alfredo Megaro[3], Antonella Cardinale[4], Jacopo Canonichesi[3], Maria De Carluccio[5,6], Roberta Mastrantonio[7], Cinzia Costa[3], Massimiliano Di Filippo[3], Alessandro Usiello[8,9], Maria Teresa Viscomi[7,10], Paolo Calabresi[5,10,13] & Alessandro Tozzi[1,13] ✉

In synucleinopathies, α-synuclein oligomers (OSyn) appear to be associated with neurodegeneration, neurotoxicity, and proinflammatory responses, even at low concentrations, suggesting their pivotal role in the pathogenesis of Parkinson's disease (PD). We utilized a rat model of synucleinopathy induced by intrastriatal injection of OSyn, aiming to elucidate events preceding the formation of fibrillary α-syn aggregates. Electrophysiological assessments and behavioral assays revealed several early alterations in OSyn rats, evident as early as 12 weeks post-OSyn injection. These included mild and variable reduction of motor activity, anxiety-like behavior, impaired bidirectional striatal long-term synaptic plasticity, and diminished spontaneous excitatory neurotransmission in the striatum. Furthermore, p-α-syn aggregates were detected in the cortex but not in the substantia nigra (SN). Confocal microscopy analysis revealed reduced vesicular glutamate transporter 1 (VGluT1) expression at striatal glutamatergic terminals. Chronic administration of the ampakine Tulrampator to OSyn animals prevented impairment of long-term depression (LTD), spontaneous striatal neurotransmission, and VGluT1 levels. Tulrampator also ameliorated the anxiety-related behavioral phenotype, albeit without attenuating motor deficits, demonstrating its efficacy in mitigating early synaptic and emotional deficits induced by OSyn. These findings provide a basis for a novel drug treatment strategy aimed at mitigating or delaying early damage at cortico-striatal terminals induced by OSyn, thereby counteracting the pathophysiological processes underlying the onset of early non-motor symptoms in PD.

Neurodegenerative diseases characterized by protein accumulation within the central nervous system (CNS) often initiate with the aggregation of small molecules, such as amyloid-β or alpha-synuclein (α-syn) proteins, which can precipitate major disorders like Alzheimer's disease and Parkinson's disease (PD)[1]. The pathophysiological processes underlying these conditions are intricate, typically initiating with synaptic and/or inflammatory events localized within specific CNS regions[2,3]. In PD, the accumulation of α-syn aggregates in the basal ganglia initiates early pathological responses at the synaptic level. Injection of α-syn pre-formed fibrils into critical structures like the nucleus striatum or the substantia nigra has been demonstrated to induce molecular, electrophysiological, and behavioral changes in rodents, mirroring the pathological features observed in human PD[2,4–6]. Within synucleinopathies, α-syn is believed to exist in a dynamic equilibrium, encompassing both α-syn oligomers (OSyn) and more aggregated forms. Oligomeric α-syn has been linked to in vivo neurodegeneration and has been shown to induce in vitro neurotoxicity and proinflammatory responses in glial cells, even at low concentrations[5,7–11]. Presently, it remains uncertain whether the neurotoxic effects exerted by α-

A full list of affiliations appears at the end of the paper. ✉e-mail: alessandro.tozzi@unipg.it

syn aggregates stem from the presence of dispersed oligomeric species, heralding the formation of fibrillary α-syn.

In synucleinopathies, synaptic structures are among the earliest targets of α-syn-induced damage[5,12,13], with OSyn emerging as the primary toxic species responsible for functional impairment[5,14,15]. Early synaptic dysfunction occurs at both cortical and subcortical levels, including impairment of noradrenergic and serotoninergic systems, and contributes to prodromal manifestations of PD such as sleep and mood disorders[16–19]. However, the precise pathophysiological mechanisms linking the presence of low molecular weight α-syn aggregates to the onset of motor and non-motor symptoms in PD remain to be fully elucidated.

To delineate the events occurring during the initial stages of α-syn spreading and evaluate the in vivo relevance of OSyn in the development of motor and non-motor symptoms, we employed a rat model induced by intrastriatal injection of OSyn (Fig. 1A, B). This model aims to capture a pathogenic scenario preceding the formation of fibrillary α-syn aggregates. Characterizing pathogenetic events in this model may offer critical insights and facilitate the identification of novel molecular targets in synucleinopathies, ameliorating the related natural progression.

Results

OSyn rats show early abnormalities of motor activity and increased anxiety-like behavior

To test whether OSyn injection affected rats' locomotion, OSyn- and sham-injected animals were tested in the open-field apparatus (Fig. 1C). OSyn-injected rats exhibited a notable reduction, albeit mild and variable, in both the mean number of sector crossings and the time spent in the center of the arena by 32.3% and 70.6%, respectively ($p < 0.05$), accompanied by a significant increase in immobility time by 260% ($p < 0.05$), compared to sham-injected animals (Fig. 1C).

No discernible differences in overall vertical activity (Fig. 1C) and grooming were observed (Fig. S1A). To further explore potential behavioral abnormalities, animals were also monitored within their home cages (Fig. 1D) (see methods). Consistently, locomotor activity was found to be compromised in OSyn rats, as evidenced by a significant 72.4% increase in immobility time compared to sham animals ($p < 0.05$). Conversely, no alterations in grooming, rearing (Fig. 1D), or sifting activities (Fig. S1B) were noted in OSyn-injected rats.

Long-term bidirectional striatal synaptic transmission is altered in OSyn-injected rats

The observed behavioral modifications in OSyn rats may stem from the direct impact of α-syn aggregates on glutamatergic synaptic function within the striatum. This impact could manifest at the postsynaptic level or by influencing terminals projecting to the striatum. Initially, we investigated potential deficits in synaptic plasticity through patch-clamp recordings of spiny projection neurons (SPNs) in the dorsolateral striatum (Fig. 2A). While no changes were noted in the basal membrane electrical properties (Fig. S2), significant modifications in both long-term potentiation (LTP) and long-term depression (LTD) were observed in OSyn rats. Specifically, LTP was reduced by 23.0% compared to sham-operated rats ($p < 0.01$, Fig. 2A), while LTD was reduced by 22.75% ($p < 0.001$, Fig. 2B).

Alpha-syn aggregates are detected in the cortex but not in the substantia nigra of OSyn rats

The observed behavioral changes and synaptic plasticity deficits in OSyn rats may be indicative of the presence of aggregated α-syn species within the brain tissue. To investigate this further, immunofluorescence analysis was performed on brain slices from OSyn and sham rats to detect potential phosphorylated α-synuclein (p-α-syn) aggregates. Results revealed the presence of p-α-syn aggregates in layer V of different cortical regions, including the motor cortex ($p < 0.05$, Figs. 2C, E and S3A) but not in the substantia nigra of OSyn rats (Fig. 2D, E), suggesting a potential impact on cortico-striatal network function. Interestingly, the absence of α-syn aggregates in the substantia nigra was associated with the lack of dopaminergic neuron loss in the substantia nigra pars compacta (SNpc) (Fig. 2F) and no alteration in the expression of the dopamine transporter at the striatal level (Fig. 2G) following striatal OSyn injection.

Cortico-striatal presynaptic terminals alteration in OSyn-injected rats

Given the potential impact of aggregated α-syn on striatal neurotransmission via modulation of synaptic neurotransmitter release, we investigated the spontaneous excitatory synaptic transmission of striatal SPNs. We found a significant decrease in the spontaneous excitatory postsynaptic currents (sEPSCs) frequency in OSyn rats (41.3% decrease) compared to sham-operated animals (OSyn vs sham, $p < 0.01$, Fig. 3A), while no changes were observed for the amplitude. Given the impairment of excitatory neurotransmission within the striatum of OSyn rats, we further examined changes in presynaptic markers associated with glutamatergic terminals. Immunostaining and densitometric quantification of VGluT1 and VGluT2 were conducted to assess potential presynaptic alterations. No significant differences in thalamic-derived VGluT2-positive terminals between OSyn rats and sham animals were found (Fig. 3B). However, immunostaining of cortical-derived VGluT1-positive terminals displayed a marked reduction of the signal intensity within the striata of OSyn rats compared to sham-operated counterparts (Fig. 3B). Interestingly, in line with our prior findings showing preserved SNpc dopaminergic neurons and the absence of α-syn aggregation in this region, immunostaining and densitometric analyses showed no differences of VGluT1 and VGluT2 levels in the SNpc between Sham and OSyn rats (Fig. S4).

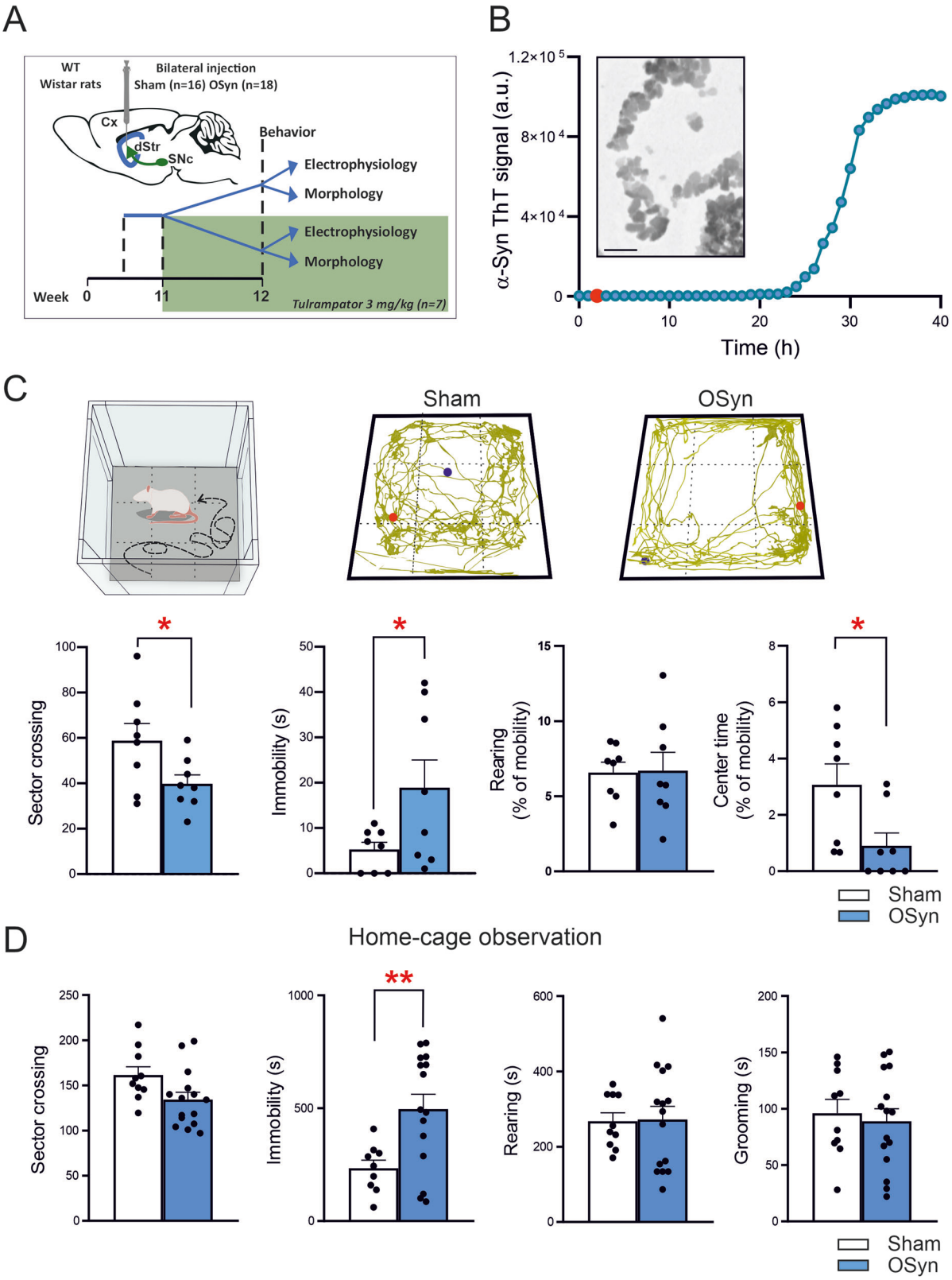
Tulrampator restored behavioral abnormalities and synaptic deficits in OSyn rats

To reverse the behavioral and synaptic alterations induced by striatal injection of OSyn, rats were chronically treated with the ampakine Tulrampator. Ampakines demonstrated neurotrophic effects and the capacity to enhance cortico-striatal connectivity[20–22]. We found that in the open-field task (Fig. 4A), OSyn rats treated with Tulrampator exhibited similar performance to sham animals in terms of time spent in the center of the arena ($p > 0.05$), suggesting that the ampakine effectively normalizes the reduced performance of OSyn rats ($p < 0.05$). However, no significant differences in sector crossings and immobility time were observed between Tulrampator-treated OSyn rats and OSyn animals ($p > 0.05$, Fig. 4A).

Whole-cell patch-clamp recordings of striatal SPNs revealed that Tulrampator treatment did not alter basal membrane electrical properties (Fig. S2), however, the treatment had no effect on LTP deficit in OSyn rats (Fig. 4B). Nevertheless, the treatment fully reestablished LTD in these animals to control levels ($p > 0.05$; OSyn vs Tulr, $p < 0.001$, Fig. 4C). Moreover, the frequency and amplitude of sEPSCs of SPNs from Tulrampator-treated OSyn rats were comparable to those of sham animals ($p > 0.05$), indicating the efficacy of the ampakine in normalizing the reduced sEPSC frequency observed in OSyn rat SPNs (Tulr vs OSyn, $p < 0.05$) (Fig. 5A). Immunofluorescence analysis of brain tissue samples from Tulrampator-treated rats further corroborated these findings, revealing a higher VGluT1 signal in Tulrampator-treated OSyn rats compared to untreated OSyn rats ($p < 0.0001$), a signal not significantly different from that measured in sham animal samples (Fig. 5B).

Discussion

The misfolding and aggregation of α-syn are recognized as key characteristics of PD. Pathological α-syn can exist in diverse conformations within the CNS, spanning from unfolded monomers to resilient fibrils. Recent investigations have elucidated the impacts of these protein aggregates at the synaptic level, demonstrating that α-syn protofibrils can initiate early synaptic dysfunction within the basal ganglia circuitry, resembling the initial phases of PD[6,23]. However, a dynamic equilibrium exists between different forms of protein[24], and unlike fibrils, oligomers are soluble and unstable, capable of interacting with lipid membranes. These distinctive characteristics render OSyn the most neurotoxic species in brain tissue[5,14,15,25]. To



elucidate the role of OSyn aggregates and their involvement in early α-synucleinopathy, a multidisciplinary approach, including electrophysiological, histological, and behavioral analyses, was conducted in an OSyn rat model.

Behavioral assessments conducted 12 weeks post-OSyn injections revealed a significant deficit in locomotor activity and increased anxiety-like behavior. Notably, these rats displayed a discernible preference for proximity to the arena walls in the open field, coupled with heightened immobility and diminished exploration, indicative of an anxiety-like state. These findings corroborate previous investigations in preclinical animal models linking α-syn aggregates to neurobehavioral alterations[6,26–29].

Fig. 1 | Graphical representation of the experimental plan; oligomers sampling time and motor behavior of OSyn rats. A Experimental plan: α-Synuclein oligomers (OSyn) or phosphate-buffered saline (PBS, Sham) are bilaterally injected into the rat striata to model early alpha-synucleinopathy. Following 12 weeks, animals undergo behavioral testing and subsequent electrophysiological and morphological assessments. The results are compared with those of animals treated with the ampakine Tulrampator. Cx cortex, dStr dorsolateral striatum, SNpc substantia nigra pars compacta. **B** Time-course graph of α-syn (1 mg/ml) aggregation in vitro as an increase in thioflavin T fluorescent staining. Inset image of the injected OSyn-containing solution (red symbol = sampling time), as visualized at the STEM (AURIGA Zeiss). Scale bar: 100 nm. **C** Schematic representation of the open-field apparatus and trajectory plots of a Sham and an OSyn rat during the open-field test. Histograms depict the distance traveled (sector crossing), immobility, rearing, and time spent in the center of the arena for OSyn and Sham rats ($n = 8$ per group). A notable decrease in the mean number of sector crossings ($t_{(14)} = 2.22$), time spent in the center of the arena ($t_{(14)} = 2.49$), and an increase in immobility time ($t_{(14)} = 2.15$) are observed in OSyn rats compared to Shams (Sham vs OSyn, $p < 0.05$). **D** Histograms illustrate home-cage observations depicting the mean number of sector crossings, immobility ($t_{(22)} = 2.92$, outliers excluded), rearing, and grooming times recorded for Sham ($n = 10$) and OSyn ($n = 15$) rats. $^{*}p < 0.05$, $^{**}p < 0.01$.

Clinical observations further validate these results, since a higher prevalence of affective symptoms is observed in PD patients compared to the general population[30,31] and point to this symptomatology as characteristic of the prodromal phase of the disease[32,33]. The reduced locomotor activity observed in OSyn rats in their active phase mirrors clinical findings in PD patients, who frequently present excessive daytime sleepiness[34–36].

The observed behavioral changes may reflect disruptions in activity-dependent plastic mechanisms that can be disrupted in the presence of toxic α-syn species[5,6,37], such as LTD and LTP, which are crucial cellular substrates for the overall function of the basal ganglia circuitry.

Accordingly, electrophysiological recordings revealed that, while the membrane properties of striatal SPNs remained unaffected in OSyn rats, both forms of long-term synaptic plasticity were abolished. This suggests that α-syn aggregates adversely affect the functional connectivity of SPNs, disrupting cortico-striatal input integration and motor coordination output, consistent with previous findings[6]. The threshold for inducing long-term synaptic plasticity in the striatum is tightly regulated by neuronal excitability of cortico-striatal glutamatergic and nigrostriatal dopaminergic pathways, which profoundly influence and modulate striatal synaptic transmission[38–41]. Injection of OSyn into the striatum may exert direct toxicity on the synaptic function of both striatal glutamatergic and dopaminergic terminals, potentially leading to retrograde transport of these aggregates to regions containing cell bodies, thereby triggering neurodegeneration. Immunofluorescence analyses reveal the presence of phosphorylated α-syn aggregates in the cortex, but not in the SNpc, emphasizing a selective vulnerability of cortico-striatal pathways at 12 weeks after injection. Moreover, the lack of dopaminergic neuron loss or dopamine transporter expression changes further underscores the specificity of the cortico-striatal axis as a primary target of OSyn pathology.

These findings align with recent studies indicating that the spread of α-syn may be influenced by both anatomical connectivity and variable α-syn expression across brain regions[42–44]. The cerebral cortex, being closer to the striatum and exhibiting higher α-syn levels than the SNpc, demonstrates pronounced susceptibility to α-syn aggregate formation and spreading[42,44]. Furthermore, OSyn displays significant synaptic toxicity, but limited seeding capacity compared to α-syn fibrils[45], making this model reflective of early disease stages.

The examination of spontaneous excitatory currents in striatal SPNs also unveiled synaptic alterations in neurotransmission. A notable decrease in the sEPSCs frequency, but not the amplitude, was observed, suggesting a presynaptic dysfunction, thus implying an unaffected number of post-synaptic receptors at excitatory synapses. Our results align with recent research demonstrating an early reduction of α-amino-3-hydroxy-5-methyl-4-isoxazole propionic acid (AMPA) receptor-mediated currents in the amygdala[46] upon striatal injection of α-syn, supporting the notion that α-syn-induced reduction of glutamatergic transmission is implicated in the appearance of neurobehavioral alterations.

The assessment of presynaptic alterations, particularly the reduced VGluT1 signal intensity, provides additional evidence of disrupted glutamatergic input from cortical neurons to striatal SPNs. At the same time, the preserved VGluT2 signal suggests that thalamic-derived inputs are less affected, reinforcing the idea of selective cortical vulnerability.

These findings are in line with recent literature suggesting that VGluT1 axon terminals are more vulnerable to α-syn pathology compared to VGluT2 axon terminals[44,46,47]. Additionally, VGlut1 and VGlut2 expressions did not differ in the SNpc, corroborating our hypothesis based on the higher vulnerability of the cortico-striatal pathway with respect to the nigrostriatal connections in the OSyn model.

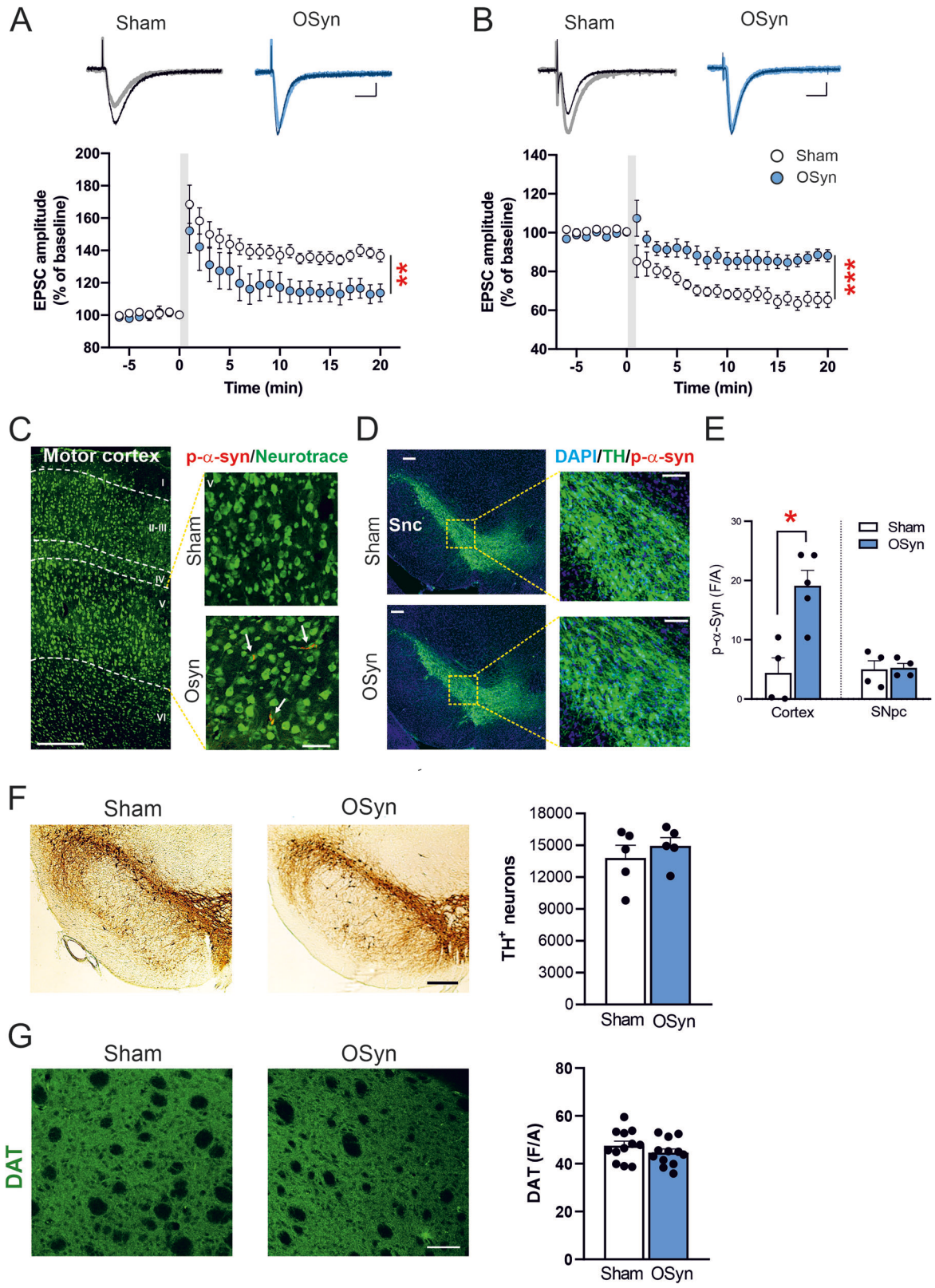
Glutamatergic synaptic transmission and plasticity heavily rely on the functioning of AMPAR, and the modulation of AMPAR activity holds the potential to enhance cognitive functions in various neurological disorders[48]. Nonetheless, inadequate pharmacological modulation often leads to adverse effects such as seizures[49–51].

Ampakines, a class of low-potency positive allosteric modulators of AMPARs, offer a safer and more applicable method for modulating AMPAR activity[52]. Ampakines stabilize the receptor within the membrane by binding to an allosteric site on the receptor, thereby augmenting its capacity to transmit excitatory signals[53]. Ampakines have demonstrated improvements in episodic and spatial working memory[54–56], display antidepressant and anxiolytic properties[57,58], and elevate levels of neurotrophic factors, particularly brain-derived neurotrophic factor (BDNF), which plays a crucial role in neuronal survival, growth, and synaptic plasticity[59–64].

The ampakine Tulrampator has been proven to enhance synaptic transmission and plasticity, showing potential in both clinical and preclinical settings for the treatment of cognitive deficits associated with various neurodegenerative and psychiatric disorders[21,52,65]. Tulrampator ameliorated electrophysiological, morphological, and anxiety-like behavioral alterations in the OSyn rat model. The open-field test revealed a reduction in anxiety-like behavior following treatment, as indicated by increased time spent in the center of the arena. Tulrampator treatment fully restored LTD of striatal SPNs and sEPSC frequency, together with normalizing presynaptic VGluT1 expression, although LTP remained impaired (Fig. 6). Our findings corroborate previous studies reporting Tulrampator's effectiveness in reversing synaptic plasticity deficits impacting both the structure and function of excitatory synapses[65]. Tulrampator was also found to exert antidepressant and anxiolytic-like effects by promoting neurogenesis and increasing levels of various neurotrophins, including BDNF[20,21]. Tulrampator did not restore LTP in OSyn rats, likely because it does not primarily affect the N-methyl-D-aspartate (NMDA) receptor nor the D1 dopamine receptor signaling cascade, both of which are compromised by α-syn aggregates and play a pivotal role in striatal SPNs LTP[5,6,37]. This aspect needs further in-depth investigation.

Overall, these findings underscore the central role of cortico-striatal dysfunction in mediating the behavioral and neurophysiological consequences of OSyn pathology. The selective vulnerability of cortical inputs and their restoration by Tulrampator suggest that enhancing cortical-striatal connectivity may be a promising therapeutic strategy. This approach could complement more conventional therapies aimed at restoring dopamine levels during the early stages of alpha-synucleinopathies. By addressing both motor and non-motor symptoms, such interventions may slow down the progression of synucleinopathy-related impairments, particularly in the prodromal phase of PD, thus greatly improving patients' quality of life.

This study was designed to investigate the early stages of α-synuclein aggregation and to evaluate the in vivo relevance of OSyn in the onset of motor and non-motor symptoms. While the model



successfully captures some early synaptic dysfunctions, it does not replicate the advanced stages of PD, as indicated by the preserved integrity of SN dopaminergic neurons and the absence of significant reductions in DAT or TH levels. Anxiety-like behavior was assessed through the open-field test, which, although a reliable first-line tool, would benefit from complementary behavioral paradigms in future studies to strengthen these findings. Moreover, the variability in mobility observed in this task may reflect early, subtle changes rather than a clear motor deficit. While a DMSO-only control group was not included in Tulrampator experiments, previous studies have demonstrated the non-toxicity of the dose used, supporting the interpretation of Tulrampator-specific effects.

Fig. 2 | Impaired striatal bidirectional long-term synaptic transmission and phospho-alpha-syn aggregates in the cortex in OSyn rats. A Representative superimposed traces of excitatory postsynaptic currents (EPSCs) recorded from spiny projection neurons (SPNs) of Sham (left) and OSyn (right) rats, both before (gray traces) and 20 min after the high-frequency stimulation (HFS) protocol (black traces) in Mg^{2+}-free artificial cerebrospinal fluid (aCSF) to induce long-term potentiation (LTP). The accompanying time-course graph depicts the average EPSC amplitude of SPNs recorded before and for 20 min after the HFS (gray band) in sham ($n = 13$) and OSyn ($n = 11$) rats. Sham vs OSyn, $t_{(22)} = 3.51$, $p < 0.01$. **B** Representative superimposed EPSC traces recorded from SPNs before (black traces) and 20 min after the HFS protocol (colored traces) to induce long-term depression (LTD) in sham (left) and OSyn (right) rats. The time-course graph displays the mean EPSC amplitude of SPNs before and for 20 min after the HFS (gray band) in Sham ($n = 12$) and OSyn ($n = 9$) animals. Sham vs OSyn, $t_{(19)} = 4.3$, $p < 0.001$. Scale bars: 50 pA and 20 ms. $^{**}p < 0.01$ and $^{***}p < 0.001$. **C** Representative coronal images of p-α-syn (red)/NeuroTraceTM 455 (green) double immunolabelling in the motor cortex of sham- and OSyn-injected rats. Scale bar: 100 µm. The insets show high magnification of layer V cortical neurons. Note the presence of p-α-syn aggregates in a representative section taken from an OSyn rat. Scale bar: 25 µm. **D** Representative midbrain images at the level of SN showing TH and p-α-syn double-immunofluorescence plus DAPI-counterstaining in sham and OSyn rats. Scale bar: 250 µm. The insets show a higher magnification of SNpc neurons. Scale bar: 50 µm. **E** Histograms of densitometric quantification of p-α-syn signal in layer V of motor cortex (M1, left) and in SNpc (right) of sham- and OSyn-injected rats expressed as mean fluorescence normalized to total layer V or SN area (F/A). Each single value represents the mean obtained by quantifying 6 samples/animal (sham, $n = 4$ rats; Osyn, $n = 5$ rats); Cortex, sham vs OSyn, $t_{(7)} = 2.5$, $p < 0.05$. **F** Representative photomicrographs of the midbrain at the level of the SN of sham- and OSyn-injected rats, showing TH-immunoreactivity. Scale bar: 100 µm. Histogram showing the number of TH+ neurons in the SNpc of sham- and OSyn-injected rats ($n = 5$ per group). **G** Representative photomicrographs of cortico-striatal sections showing DAT immunostainings in the striatum of sham and OSyn rats. Scale bar: 50 µm. Histogram showing optical density (F/A) of DAT signal in the striatum of sham- and OSyn-injected rats. Quantification was done on 12 samples per rat ($n = 6$ per group).

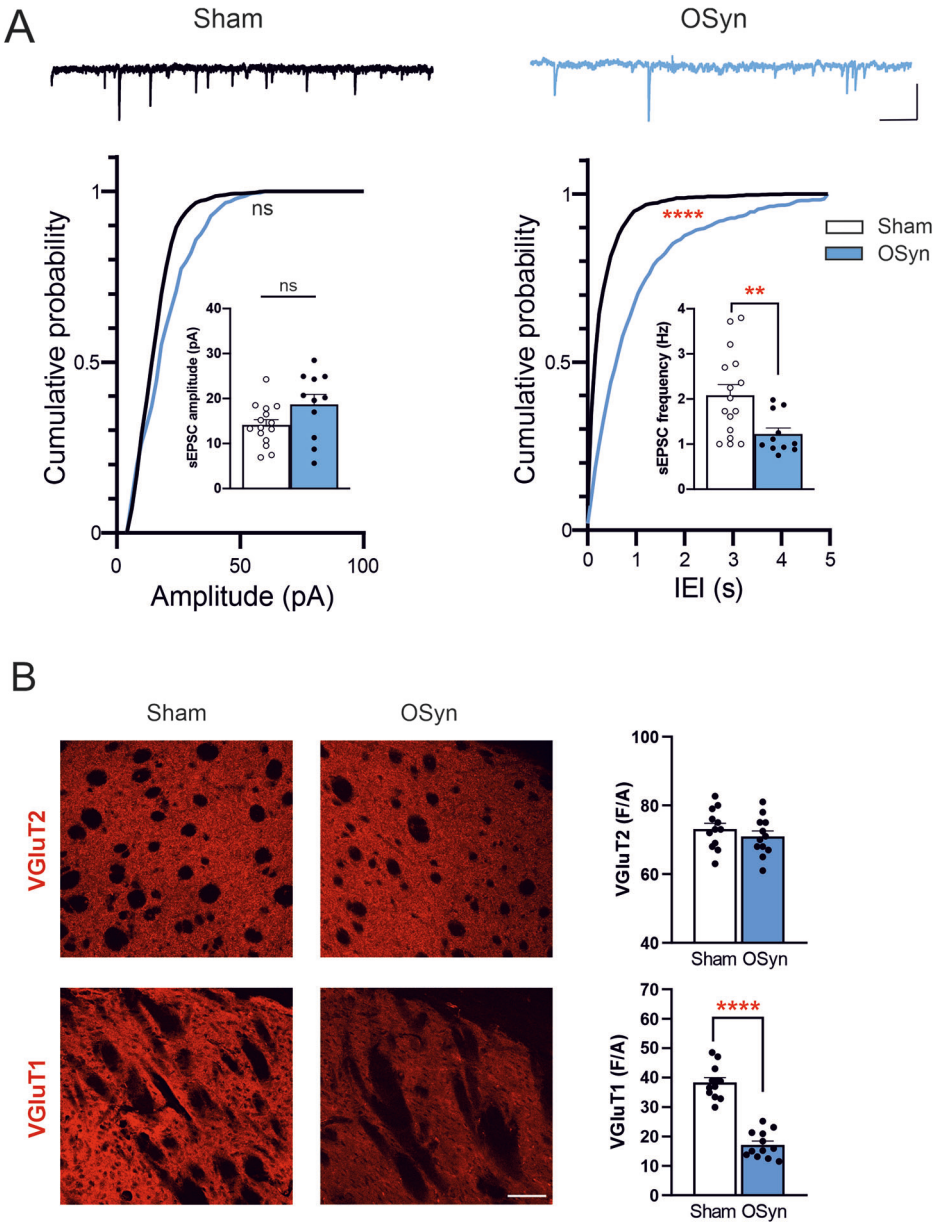


Fig. 3 | OSyn-injected rats exhibit diminished spontaneous excitatory synaptic transmission in the striatum, along with a decrease in VGluT1 immunostaining, while the signal for VGluT2 remains unchanged. A Representative traces of sEPSCs and cumulative probability graphs depicting the amplitude (left) and inter-event interval (IEI, right) of sEPSCs recorded in striatal SPNs of sham and OSyn-injected rats. Insets show bar plots indicating the mean sEPSC amplitude (left) and frequency (right) of recorded events. Sham ($n = 16$) vs OSyn ($n = 11$), IEI: $D = 0.6$, $p < 0.0001$; frequency: $t_{(25)} = 2.80$, $p < 0.01$. Scale bar: 20 pA, 1 s. **B** Representative microphotographs of VGluT1 and VGluT2 immunostainings in the striatum of sham and OSyn-injected rats. Scale bars: 50 µm. Histogram of the optical density (F/A) of VGluT2 and VGluT1 signals in the striatum of sham and OSyn rats. Quantification was performed at the dorsomedial level of the striatum, analyzing 12 samples per rat ($n = 6$ rats per group). $^{**}p < 0.01$; $^{****}p < 0.0001$.

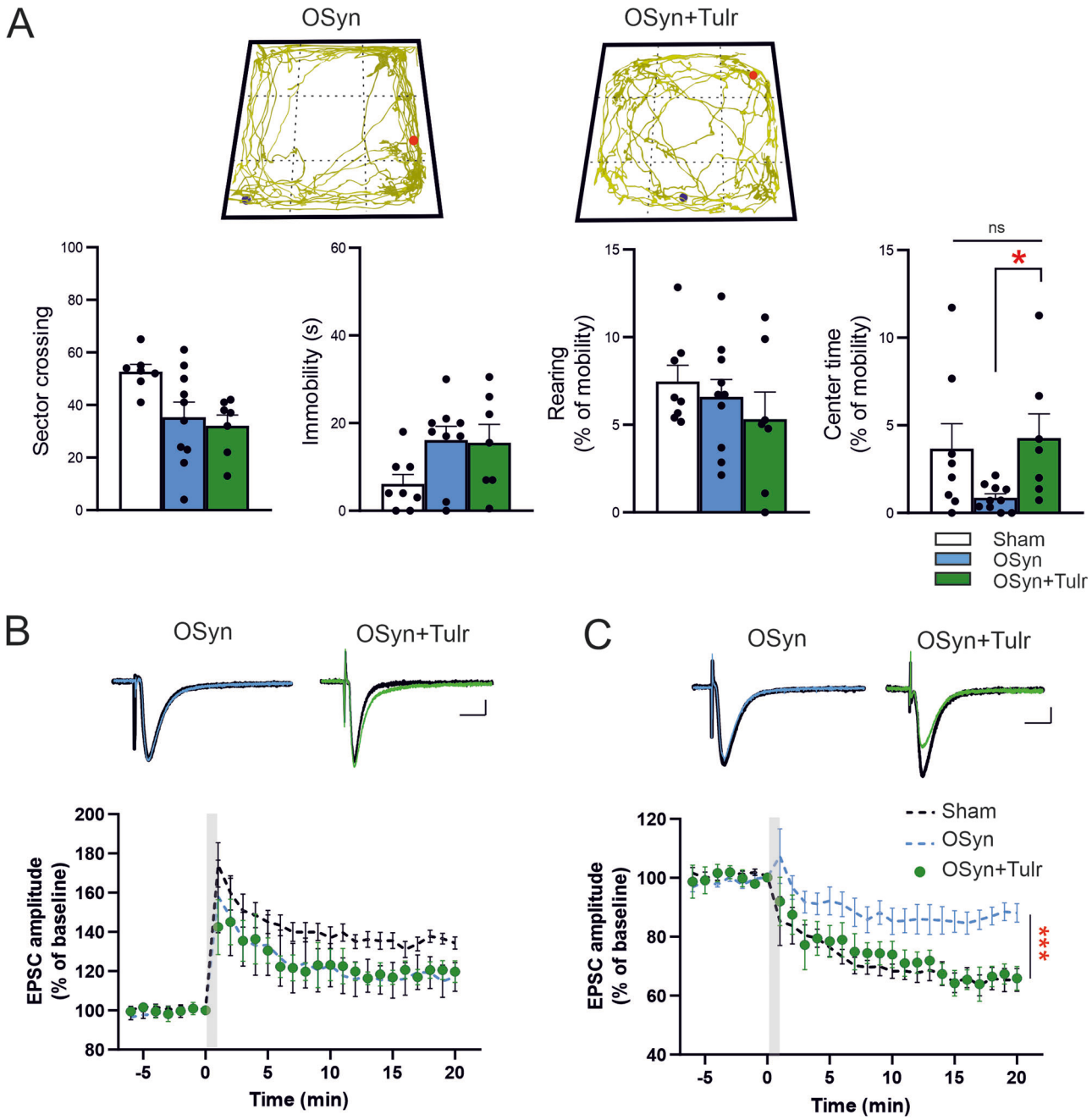


Fig. 4 | Tulrampator treatment reversed behavioral abnormalities and restored LTD deficits in OSyn-injected rats. A Track plots depicting the movement trajectories of OSyn and Tulrampator-treated OSyn rats during the open-field test. Histograms illustrating the distance traveled, immobility, rearing, and time spent at the center of the arena for sham ($n = 8$), OSyn-injected ($n = 10$), and Tulrampator-treated OSyn ($n = 7$) groups; (Time at center, OSyn vs Tulr, $t_{(15)} = 2.86$, $p < 0.05$); outliers were excluded. **B** Representative superimposed EPSC traces recorded from SPNs of OSyn and Tulrampator-treated OSyn rats, before (black traces) and 20 min after the HFS protocol in magnesium-free solution (colored traces) to induce LTP. Time-course graphs depicting the EPSP amplitude of SPNs before and for 20 min after the HFS protocol (gray band) ($n = 6$) from Tulr-treated OSyn rats. **C** Representative superimposed EPSC traces recorded from SPNs of OSyn and Tulrampator-treated OSyn rats, before (black traces) and 20 min after the HFS protocol (colored traces) to induce LTD. Time-course graphs depicting the EPSP amplitude of SPNs before and for 20 min after the HFS protocol (gray band) ($n = 8$) from Tulr-treated OSyn rats. It is noteworthy that the time-course plot overlaps with that of OSyn for LTP (left) and with that of sham animals for LTD (right). LTD, Sham vs Tulr, $p > 0.05$; Tulr vs OSyn, $t_{(15)} = 4.43$, $p < 0.001$. Scale bars: 50 pA, 20 ms, $^{*}p < 0.05$; $^{***}p < 0.001$.

The detection of p-α-syn in the cortex supports a pattern of local accumulation following OSyn injection; however, we recognize that the extent of α-synuclein aggregation observed may exceed what is typically reported in prodromal PD brains. A potential confounding effect related to the injection route of OSyn cannot be fully excluded. Our data support the idea that p-α-syn accumulation alone can affect cortico-striatal function. However, we acknowledge that a causal link between this dysfunction and prodromal anxiety-like symptoms in PD remains to be clearly established, and further studies are needed to explore this potential relationship.

Finally, the lack of LTP restoration by Tulrampator suggests that additional mechanisms beyond AMPAR modulation may be involved, an avenue worth exploring in future work.

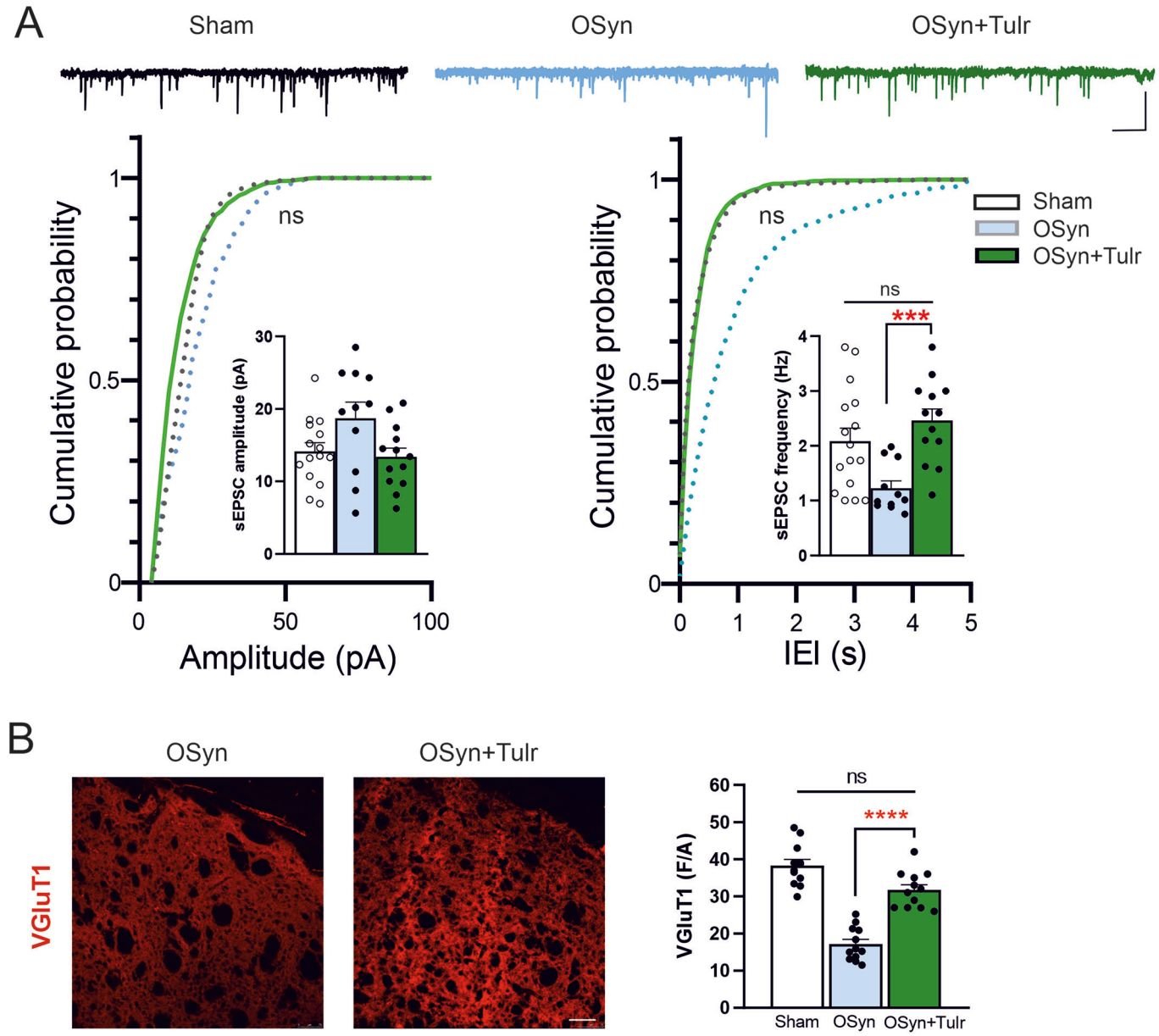


Fig. 5 | Rescue of spontaneous excitatory synaptic transmission in Tulrampator-treated OSyn rats. A Representative sEPSC traces and cumulative probability graphs depicting the amplitude (left) and the inter-event interval (IEI, right) of sEPSCs recorded in striatal SPNs of Tulrampator-treated OSyn rats ($n = 14$). The insets present bar plots illustrating the mean sEPSC amplitude (left) and frequency (right) of the recorded events. Notably, the cumulative plot of the Tulrampator-treated OSyn group overlaps with that of the sham group for both amplitude and frequency ($p > 0.05$), with no significant difference observed in sEPSC frequency compared to the sham group ($p > 0.05$). Tulrampator-treated OSyn vs OSyn, IEI, $D = 0.68$, $p < 0.0001$; frequency, $t_{(22)} = 4.73$, $p < 0.001$. Scale bar: 20 pA, 1 s. **B** Representative microphotographs depicting VGluT1 immunostaining in the striatum of OSyn and Tulrampator-treated OSyn rats. Scale bar: 50 µm. Histogram of the optical density (F/A) of the VGluT1 signal in the striatum of Sham, OSyn, and Tulrampator-treated OSyn rats. Quantification of 12 samples/rat ($n = 6$ rats per group); OSyn vs OSyn-Tulr, $t_{(22)} = 7.59$, $p < 0.0001$. ***$p < 0.001$; ****$p < 0.0001$.

Methods

Male adult rats received bilateral injections of oligomeric α-synuclein (OSyn rats) or phosphate-buffered saline (PBS, sham rats) into the dorsal striatum. Subsequently, behavioral phenotypes were assessed, and the rats were sacrificed for immunohistochemical and electrophysiological recordings. Additionally, one cohort of animals received treatment with the ampakine Tulrampator before the behavioral, immunohistochemical, and electrophysiological analyses (Fig. 1A). Rats underwent the open-field test 40 min after the last systemic injection of Tulrampator and were then sacrificed for electrophysiological recordings or processed for subsequent immunohistochemical analyses.

Animals

Male adult Wistar rats (Charles River Laboratories) weighing 250–275 g at the beginning of the experiments were utilized. This study was designed and reported in accordance with the ARRIVE guidelines for animal research. All procedures involving live animals were performed in accordance with the guidelines outlined in the European Directive 2010/63/EU and were approved by the Animal Care and Use Committee at the University of Perugia (Italy), as well as the Italian Ministry of Health (N.75/2021-PR). The animals were housed in two per cage with free access to water and food and were kept under constant temperature, humidity, and a 12 h light/dark cycle. Rats were allocated randomly to various experimental groups.

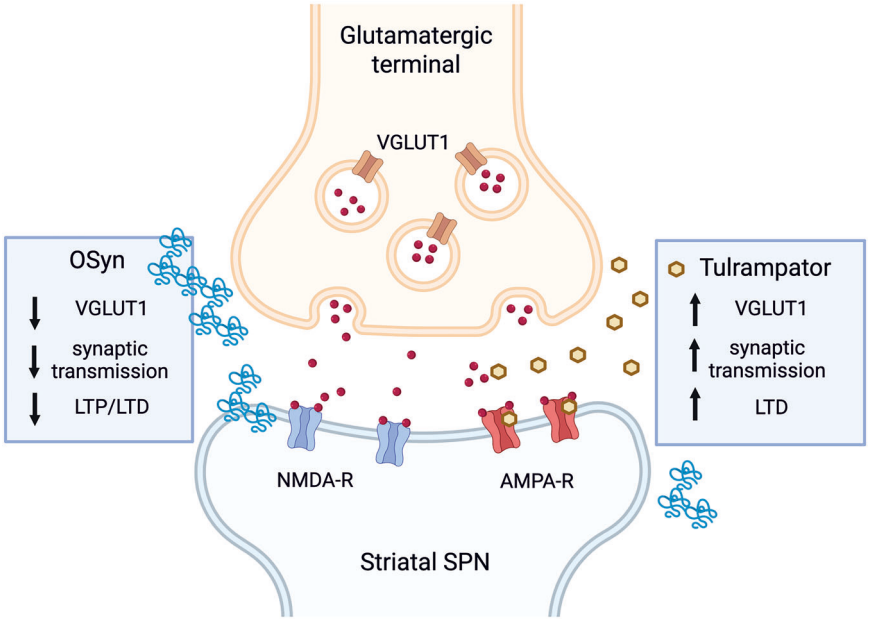


Fig. 6 | Schematic representation of a cortico-striatal synapse affected by oligomeric α-synuclein and the pharmacological action of Tulrampator. Illustration of a cortico-striatal synapse in which oligomeric α-synuclein (OSyn) reduces VGluT1 levels, impairs synaptic transmission, and causes deficits in long-term potentiation (LTP) and depression (LTD), while treatment with the ampakine Tulrampator restores VGluT1 expression, normal synaptic transmission, and LTD.

Experimenters were blinded to the experimental group assignments during data collection.

Preparation of α-syn-oligomers

Lyophilized monomeric α-syn (recombinant human α-syn, Sigma Aldrich) was dissolved in sterile PBS to a final concentration of 1 mg/ml (70 µm). α-Syn oligomers were generated by continuous shaking (600 rpm) at 37 °C for 2 h. The aggregation process was monitored by thioflavin T assay in a CLARIOstar reader (BMG LABTECH). Oligomer formation was confirmed by scanning transmission electron microscopy (STEM) (AURIGA Zeiss) (Fig. 1B). At the end of this procedure, α-Syn oligomer aliquots were stored at −80 °C until used for intracerebral injection. Endotoxin levels were measured to be 0.0045 EU/µg of protein using the Limulus Amebocyte Lysate endotoxin assay (Thermo Scientific).

Surgery

Surgical procedures were conducted on deeply anesthetized rats aged 7–8 weeks [using Zoletil 20 mg/kg combined with xylazine 9 mg/kg, administered intraperitoneally (i.p.)]. The animals received two bilateral intrastriatal injections (1 µl at each site) of either OSyn (1 mg/ml dissolved in PBS) or PBS. Stereotaxic striatal injection coordinates, referenced with a tooth bar set at 0.00, were as follows: (i) anteroposterior (AP) + 1.0, mediolateral (ML) + 3.0, dorsoventral (DV) −5.0; and (ii) AP + 1.0, ML −3.0, DV −5.0[6]. Following the surgical procedure, the animals were monitored until fully awake and then returned to their cages. Twelve weeks post-surgery, the animals underwent behavioral tests, electrophysiological assessments, and morphological analyses.

Subchronic Tulrampator treatment

Tulrampator (also known as s-47445) was prepared at the working concentration by diluting it in a suspension containing dimethyl sulfoxide (DMSO) at 10%, polyethylene glycol 300 (PEG 300) at 40%, Tween 80 at 5%, and saline at 45%, following the manufacturer's instructions for in vivo treatment (MedChemExpress, CAS no. 1038984-31-4). The suspension contained 100 µl/kg DMSO, a dose known to be well below the maximum tolerated dose for rats (5 ml/kg, chronic administration) and not to cause harm, inflammation, or affect locomotor activity[66]. Although the DMSO concentration was within a range not associated with behavioral or synaptic alterations, the absence of a vehicle-treated group should be considered. Rats at 11 weeks post-surgery were then administered Tulrampator via i.p. injection at a dosage of 3 mg/kg daily for 1 week. Subsequently, the rats underwent behavioral tests, after which they were euthanized, and brain tissue samples were collected for electrophysiological recordings and morphological analyses.

Behavioral assessment

Animals underwent open-field test and home-cage observation at 12 weeks post-OSyn or PBS injection. Behavioral assessments were conducted consistently within the same room and at the same time of day, administered by an investigator blinded to the rat's condition. The behavior was manually scored by blinded operators using timing recording software (ODLog, Macropod Software). General locomotor activity was evaluated using the open-field task, which involved a 10-min habituation followed by a 10-min testing period during the animals' active phase, as previously described[6].

Additionally, rats were observed within their home cages, maintained under standard housing conditions (12:12 h light/dark cycle, lights on at 7 a.m., room temperature maintained at 23 °C, with food and water *ad libitum*), during 1-h sessions conducted within the animals' active phase (7:30–9:30 p.m.). In order to best monitor behavior, the animals were housed individually.

Immunohistochemistry

Rats were euthanized following deep sedation. Upon dissection, the brains were fixed in 4% paraformaldehyde (PFA) (Sigma Aldrich) at 4 °C for a minimum of 24 h, then transferred to a PBS solution containing 30% sucrose and 0.02% sodium azide and stored at 4 °C for at least another 24 h or until sectioning. Brain sections (30 µm thick) were obtained using a cryostat (Leica CM1900) and stored in PBS containing 0.02% sodium azide at 4 °C until subsequent histological procedures.

For immunohistochemistry, primary and secondary antibody solutions, as well as ExtrAvidin solutions, were prepared in PB containing 0.3% Triton X-100. Each incubation step was followed by 5-min rinses in PB, repeated three times. For immunoperoxidase staining, sections were treated with 0.3% H2O2 for 5 min to block endogenous peroxidase activity. Subsequently, they were incubated for 48 h at 4 °C with a solution containing a mouse anti-tyrosine hydroxylase (TH) antibody (1:1000, Sigma Aldrich; MAB318), followed by a 2-h incubation with a biotinylated donkey anti-mouse antibody (1:200, Jackson Immunoresearch). The sections were then incubated for another 2 h in an ExtrAvidin solution (1:1000; Sigma Aldrich), and 3,3′-diaminobenzidine (DAB) 0.05% was used as the chromogen.

Finally, sections were mounted on chrome-alum-coated slides, air-dried, dehydrated, and coverslipped.

For immunofluorescence staining, sections were incubated overnight at 4 °C with primary antibodies, including rabbit anti-phosphorylated α-syn (phosphoS129; 1:100; Abcam; #ab51253) and mouse anti-tyrosine hydroxylase (1:1000; Sigma Aldrich; MAB318), in PBS containing 0.1% bovine serum albumin (BSA) and 0.3% Triton X-100. Subsequently, the sections were incubated for 2 h with a cocktail of secondary antibodies, including Alexa Fluor 555 donkey anti-rabbit IgG and Alexa Fluor 488 donkey anti-mouse IgG (1:200; Invitrogen). Neuronal cells were counterstained with DAPI or NeuroTrace™ 455 green fluorescent Nissl-Stain. Confocal images were acquired using a Nikon Confocal Microscope (NIKON TiE2). Additionally, brain sections were incubated with guinea pig anti-vesicular glutamate transporter 1 (VGluT1; 1:800, Synaptic System; #135304), guinea pig anti-vesicular glutamate transporter 2 (VGluT2; 1:800, Synaptic System; #135404), and anti-dopamine transporter (DAT, 1:1000; Sigma Aldrich; MAB369) antibodies. After washing, the sections were incubated for 2 h at room temperature with secondary antibodies, including Alexa Fluor 555 donkey anti-guinea pig IgG and Alexa Fluor 488 donkey anti-rat IgG (1:200; ThermoFisher Scientific). Subsequently, the sections were mounted using an anti-fade medium (Fluoromount; Sigma) and examined under a confocal laser-scanning microscope (NIKON TiE2). The specificity of immunohistochemical labeling was confirmed by the omission of primary antibodies and the use of normal serum instead (negative controls).

Stereological analysis

The analysis of SNpc was performed on brain sections from five animals per group. The SNpc was outlined using the 4× objective, while the 100X oil immersion objective was used for neuronal cell count. A Stereo Investigator System (MicroBrightField Europe e.K., Magdeburg, Germany) that included a three-dimensional optical fractionator counting probe (x, y, z dimension of 50 × 50 × 10 µm, respectively) was used to obtain an unbiased estimation of total TH-positive cells, according to published procedures[23]. For each animal, 10 sections, covering the rostro-caudal extension of the SNpc, were counted. Data collection for stereology was done by researchers blind to the experimental group being analyzed.

Densitometric analysis of fluorescence images

Densitometric analysis of DAT, VGluT1, and VGluT2 was performed on rat brain sections. To avoid staining variability among sections and experimental groups, sections were incubated with the same cocktail of primary and secondary antibodies at the same time. Furthermore, the confocal settings for image capture were kept constant throughout the acquisition of sections from both groups of rats. After confocal, images were exported in TIFF and analyzed with ImageJ software (http://rsb.info.nih.gov/ij/; National Institutes of Health). The background signal for antibodies was determined in a non-stained area, and the threshold was adjusted according to the background signal and kept constant between sections. DAT, VGluT1- and VGluT2-associated signals were quantified by manually outlining the striatum and the SNpc. Mean signal intensities (F) of VGluT1 or VGluT2 were measured on 2 squared frames (150 × 150 µm for the striatum and 100 × 100 µm for the SNpc). The frames were pseudo-randomly distributed, medio-laterally on 6 striatal and SN sections, one every 250 µm, sampled in each rat to cover the rostro-caudal extent of these brain structures entirely[67]. The F/A ratio defines the mean fluorescence of individual samples (F) normalized to the total cellular surface (A). Accordingly, quantification was done on 12 samples per rat (Sham, $n = 4$ and OSyn, $n = 5$). Data collection for densitometry was done by researchers blind to the group analyzed.

Electrophysiology

Rats were euthanized by decapitation 12 weeks post-surgery, and 220 µm-thick cortico-striatal coronal brain slices were prepared using a vibratome. Slices were maintained in artificial cerebrospinal fluid (aCSF), which was continuously bubbled with a 95% O_2–5% CO_2 gas mixture at room temperature. The composition of the aCSF included: 126 mM NaCl, 2.5 mM KCl, 1.2 mM $MgCl_2$, 1.2 mM NaH_2PO_4, 2.4 mM $CaCl_2$, 10 mM glucose, and 25 mM $NaHCO_3$[6]. Single slices were then transferred to a recording chamber and submerged in a continuously flowing aCSF (34 °C; flow rate: 2.5–3 ml/min), also bubbled with a 95% O_2–5% CO_2 gas mixture.

Whole-cell patch-clamp recordings were conducted from SPNs that were visualized using infrared differential interference contrast microscopy (Olympus) in the dorsal striatum. Only SPNs selected on the basis of their intrinsic membrane properties were included in the study. The whole-cell patch-clamp recordings (with access resistance of 15–30 MΩ and a holding potential of −80 mV) were performed using borosilicate pipettes (4–7 MΩ) filled with an internal solution consisting of: 145 m MK^+-gluconate, 0.1 mM $CaCl_2$, 2 mM $MgCl_2$, 0.1 mM EGTA, 10 mM HEPES, 0.3 mM Na-GTP, and 2 mM Mg-ATP, adjusted to pH 7.3 with KOH. sEPSCs were recorded for 5 min. Signals were low-pass filtered at 0.1 kHz, digitized at 5 kHz using Clampex 10 software, analyzed offline using automated event detection algorithms, and subsequently checked manually for accuracy. A bipolar electrode, connected to a stimulation unit, was positioned in the white matter between the cortex and the striatum to stimulate glutamatergic fibers (at 0.1 Hz) and evoke excitatory postsynaptic currents (EPSCs), while the recording electrode was positioned in the dorsolateral striatum. Following stable recording of evoked EPSCs for at least 10 min, a high-frequency stimulation protocol (HFS) was applied, comprising three trains of 3 s each (with 20-s intervals), delivered at 100 Hz to induce LTP or LTD. External Mg^{2+} ions were omitted from the solution to enhance the contribution of NMDA receptors during LTP experiments[6]. Additionally, 50 mM picrotoxin was added to the aCSF in all patch-clamp experiments to block $GABA_A$ receptors.

Statistical analysis

The sample size calculation (rats required) was performed in advance using G*Power3 software, with power and confidence levels set to 80% and 95%, respectively, while estimating effect magnitude and standard deviation. Statistical analyses were conducted using GraphPad Prism 8.0 (GraphPad Software, USA). For behavioral assessments, Student's t-test for unpaired samples was employed. The number of experiments (n) represents the total number of animals tested in each experimental group. In the open-field test, data were acquired for a 10-min time frame (Table S1), however, to evaluate the steady-state exploratory behavior, data from the last 5 min of the sessions were presented. To minimize motor-related confounds, center time and rearing were normalized to effective mobility (total time minus immobility) prior to statistical analysis. The presence of statistical outliers was assessed using the Grubbs' test ($\alpha = 0.05$); outliers were excluded prior to statistical analysis.

Immunostaining data were subjected to analysis using a two-tailed Student's t-test. In electrophysiological recordings, the intrinsic electric membrane properties of striatal SPNs were assessed for differences among groups using one-way ANOVA. Changes in EPSC amplitude induced by stimulation protocols were expressed as a percentage of the baseline, with the baseline representing the normalized EPSC mean amplitude acquired during a stable period (10–15 min) before stimulation. The presence of LTP or LTD was verified in each experiment using Student's t-test for unpaired samples, comparing the mean EPSC amplitude recorded during the last minute ($t = 20$). Cumulative probability curves depicted in the figures were generated by pooling together the amplitude of spontaneous EPSCs (sEPSCs) and their inter-event intervals (IEIs) for each group, with the Kolmogorov–Smirnov test used to compare probability distributions. Mean sEPSC amplitudes and frequencies were compared using unpaired Student's t-tests. The number (n) of experiments for electrophysiological recordings represented the number of recorded neurons. Results in the text and graphs presented in the figures are reported as mean ± standard error of the mean, with statistical significance set at $p < 0.05$.

Data availability

Data are provided within the manuscript or supplementary information files.

Received: 14 January 2025; Accepted: 12 July 2025;
Published online: 29 July 2025

References

1. Soto, C. & Pritzkow, S. Protein misfolding, aggregation, and conformational strains in neurodegenerative diseases. *Nat. Neurosci.* **21**, 1332–1340 (2018).
2. Calabresi, P., Di Lazzaro, G., Marino, G., Campanelli, F. & Ghiglieri, V. Advances in understanding the function of alpha-synuclein: implications for Parkinson's disease. *Brain J. Neurol.* **146**, 3587–3597 (2023).
3. Bellingacci, L., Canonichesi, J., Mancini, A., Parnetti, L. & Di Filippo, M. Cytokines, synaptic plasticity and network dynamics: a matter of balance. *Neural Regen. Res.* **18**, 2569–2572 (2023).
4. Björklund, A., Nilsson, F., Mattsson, B., Hoban, D. B. & Parmar, M. A combined α-synuclein/fibril (SynFib) model of Parkinson–like synucleinopathy targeting the nigrostriatal dopamine system. *J. Parkinson's Dis* **12**, 2307–2320 (2022).
5. Durante, V. et al. Alpha-synuclein targets GluN2A NMDA receptor subunit causing striatal synaptic dysfunction and visuospatial memory alteration. *Brain J. Neurol.* **142**, 1365–1385 (2019).
6. Tozzi, A. et al. Dopamine-dependent early synaptic and motor dysfunctions induced by α-synuclein in the nigrostriatal circuit. *Brain* **144**, 3477–3491 (2021).
7. Winner, B. et al. In vivo demonstration that alpha-synuclein oligomers are toxic. *Proc. Natl. Acad. Sci. USA***108**, 4194–4199 (2011).
8. Kalia, L. V., Kalia, S. K., McLean, P. J., Lozano, A. M. & Lang, A. E. α-Synuclein oligomers and clinical implications for Parkinson disease. *Ann. Neurol.* **73**, 155–169 (2013).
9. Cascella, R. et al. The release of toxic oligomers from α-synuclein fibrils induces dysfunction in neuronal cells. *Nat. Commun.* **12**, 1814 (2021).
10. Pirhaghi, M. et al. A penetratin-derived peptide reduces the membrane permeabilization and cell toxicity of α-synuclein oligomers. *J. Biol. Chem.* **298**, 102688 (2022).
11. Ahmadi Rastegar, D. et al. Effect of LRRK2 protein and activity on stimulated cytokines in human monocytes and macrophages. *npj Parkinson's Dis* **8**, 34 (2022).
12. Calo, L., Wegrzynowicz, M., Santivañez-Perez, J. & Grazia Spillantini, M. Synaptic failure and α-synuclein. *Mov. Disord.***31**, 169–177 (2016).
13. Imbriani, P., Schirinzi, T., Meringolo, M., Mercuri, N. B. & Pisani, A. Centrality of early synaptopathy in Parkinson's disease. *Front. Neurol.* **9**, 103 (2018).
14. Mj, D. et al. Extracellular alpha-synuclein oligomers modulate synaptic transmission and impair LTP via NMDA-receptor activation. *J. Neurosci.***32**, 11750–11762 (2012).
15. Ferreira, D. G. et al. α-synuclein interacts with PrPC to induce cognitive impairment through mGluR5 and NMDAR2B. *Nat. Neurosci.* **20**, 1569–1579 (2017).
16. Kulkarni, A. S., Burns, M. R., Brundin, P. & Wesson, D. W. Linking α-synuclein-induced synaptopathy and neural network dysfunction in early Parkinson's disease. *Brain Commun.* **4**, fcac165 (2022).
17. Delaville, C. et al. Emerging dysfunctions consequent to combined monoaminergic depletions in Parkinsonism. *Neurobiol. Dis.* **45**, 763–773 (2012).
18. Kim, S., Woo, K. A., Choi, H., Shin, J. H. & Kim, H.-J. Monoaminergic degeneration, cognition, and autonomic symptom trajectory in early Parkinson's disease. *Park. Relat. Disord.* **127**, 107086 (2024).
19. Canonichesi, J., Bellingacci, L., Rivelli, F. & Tozzi, A. Enhancing sleep quality in synucleinopathies through physical exercise. *Front. Cell. Neurosci.* **19**, 1515922 (2025).
20. Calabrese, F. et al. Upregulation of neurotrophins by S 47445, a novel positive allosteric modulator of AMPA receptors in aged rats. *Pharmacol. Res.* **121**, 59–69 (2017).
21. Mendez-David, I. et al. S 47445 produces antidepressant- and anxiolytic-like effects through neurogenesis dependent and independent mechanisms. *Front. Pharmacol.* **8**, 462 (2017).
22. Zeng, F. et al. AMPAkines potentiate the corticostriatal pathway to reduce acute and chronic pain. *Mol. Brain* **14**, 45 (2021).
23. Marino, G. et al. Intensive exercise ameliorates motor and cognitive symptoms in experimental Parkinson's disease restoring striatal synaptic plasticity. *Sci. Adv.* **9**, eadh1403 (2023).
24. Alam, P., Bousset, L., Melki, R. & Otzen, D. E. α-synuclein oligomers and fibrils: a spectrum of species, a spectrum of toxicities. *J. Neurochem.* **150**, 522–534 (2019).
25. Fusco, G. et al. Structural basis of membrane disruption and cellular toxicity by α-synuclein oligomers. *Science* **358**, 1440–1443 (2017).
26. Stoyka, L. E. et al. Behavioral defects associated with amygdala and cortical dysfunction in mice with seeded α-synuclein inclusions. *Neurobiol. Dis.* **134**, 104708 (2020).
27. Yun, S. P. et al. Block of A1 astrocyte conversion by microglia is neuroprotective in models of Parkinson's disease. *Nat. Med.* **24**, 931–938 (2018).
28. Burtscher, J. et al. Chronic corticosterone aggravates behavioral and neuronal symptomatology in a mouse model of alpha-synuclein pathology. *Neurobiol. Aging* **83**, 11–20 (2019).
29. Karampetsou, M. et al. Phosphorylated exogenous alpha-synuclein fibrils exacerbate pathology and induce neuronal dysfunction in mice. *Sci. Rep.* **7**, 16533 (2017).
30. Weintraub, D. et al. The neuropsychiatry of Parkinson's disease: advances and challenges. *Lancet Neurol.* **21**, 89–102 (2022).
31. Broen, M. P. G., Narayen, N. E., Kuijf, M. L., Dissanayaka, N. N. W. & Leentjens, A. F. G. Prevalence of anxiety in Parkinson's disease: a systematic review and meta-analysis. *Mov. Disord.***31**, 1125–1133 (2016).
32. Jacob, E. L., Gatto, N. M., Thompson, A., Bordelon, Y. & Ritz, B. Occurrence of depression and anxiety prior to Parkinson's disease. *Park. Relat. Disord.* **16**, 576 (2010).
33. Postuma, R. B. & Berg, D. Prodromal Parkinson's disease: the decade past, the decade to come. *Mov. Disord.* **34**, 665–675 (2019).
34. Arnulf, I., Leu, S. & Oudiette, D. Abnormal sleep and sleepiness in Parkinson's disease. *Curr. Opin. Neurol.* **21**, 472–477 (2008).
35. Whitehead, D. L., Davies, A. D. M., Playfer, J. R. & Turnbull, C. J. Circadian rest-activity rhythm is altered in Parkinson's disease patients with hallucinations. *Mov. Disord.***23**, 1137–1145 (2008).
36. Hunt, J. et al. Sleep and circadian rhythms in Parkinson's disease and preclinical models. *Mol. Neurodegener.* **17**, 2 (2022).
37. Tozzi, A. et al. Alpha-synuclein produces early behavioral alterations via striatal cholinergic synaptic dysfunction by interacting with GluN2D N-methyl-D-aspartate receptor subunit. *Biol. Psychiatry* **79**, 402–414 (2016).
38. Calabresi, P., Maj, R., Pisani, A., Mercuri, N. B. & Bernardi, G. Long-term synaptic depression in the striatum: physiological and pharmacological characterization. *J. Neurosci.***12**, 4224–4233 (1992).
39. Calabresi, P., Picconi, B., Tozzi, A. & Di Filippo, M. Dopamine-mediated regulation of corticostriatal synaptic plasticity. *Trends Neurosci.* **30**, 211–219 (2007).
40. Centonze, D., Picconi, B., Gubellini, P., Bernardi, G. & Calabresi, P. Dopaminergic control of synaptic plasticity in the dorsal striatum. *Eur. J. Neurosci.* **13**, 1071–1077 (2001).
41. Di Filippo, M. et al. Short-term and long-term plasticity at corticostriatal synapses: implications for learning and memory. *Behav. Brain Res.* **199**, 108–118 (2009).
42. Henderson, M. X. et al. Spread of α-synuclein pathology through the brain connectome is modulated by selective vulnerability and predicted by network analysis. *Nat. Neurosci.* **22**, 1248–1257 (2019).

43. Awa, S. et al. Phosphorylation of endogenous α-synuclein induced by extracellular seeds initiates at the pre-synaptic region and spreads to the cell body. *Sci. Rep.* **12**, 1163 (2022).
44. Erskine, D. et al. Regional levels of physiological α-synuclein are directly associated with Lewy body pathology. *Acta Neuropathol.***135**, 153–154 (2018).
45. Froula, J. M. et al. Defining α-synuclein species responsible for Parkinson's disease phenotypes in mice. *J. Biol. Chem.* **294**, 10392–10406 (2019).
46. Chen, L. et al. Synaptic location is a determinant of the detrimental effects of α-synuclein pathology to glutamatergic transmission in the basolateral amygdala. *eLife* **11**, e78055 (2022).
47. Vasili, E. et al. Endogenous levels of alpha-synuclein modulate seeding and aggregation in cultured cells. *Mol. Neurobiol.* **59**, 1273–1284 (2022).
48. Arai, A. C. & Kessler, M. Pharmacology of ampakine modulators: from AMPA receptors to synapses and behavior. *Curr. Drug Targets* **8**, 583–602 (2007).
49. Rogawski, M. A. & Donevan, S. D. AMPA receptors in epilepsy and as targets for antiepileptic drugs. *Adv. Neurol.* **79**, 947–963 (1999).
50. Rogawski, M. A. AMPA receptors as a molecular target in epilepsy therapy. *Acta Neurol. Scand. Suppl*. 9–18 (2013).
51. Eiro, T. et al. Dynamics of AMPA receptors regulate epileptogenesis in patients with epilepsy. *Cell Rep. Med.* **4**, 101020 (2023).
52. Kadriu, B. et al. Positive AMPA receptor modulation in the treatment of neuropsychiatric disorders: a long and winding road. *Drug Discov. Today* **26**, 2816–2838 (2021).
53. Lynch, G. Glutamate-based therapeutic approaches: ampakines. *Curr. Opin. Pharmacol.* **6**, 82–88 (2006).
54. O'Neill, M. J. & Dix, S. AMPA receptor potentiators as cognitive enhancers. *IDrugs Investig. Drugs J.* **10**, 185–192 (2007).
55. O'Neill, M. J., Bleakman, D., Zimmerman, D. M. & Nisenbaum, E. S. AMPA receptor potentiators for the treatment of CNS disorders. *Curr. Drug Targets CNS Neurol. Disord.* **3**, 181–194 (2004).
56. Black, M. D. Therapeutic potential of positive AMPA modulators and their relationship to AMPA receptor subunits. A review of preclinical data. *Psychopharmacology***179**, 154–163 (2005).
57. Lauterborn, J. C. et al. Chronic Ampakine Treatments Stimulate Dendritic Growth and Promote Learning in Middle-Aged Rats. *J. Neurosci.* **36**, 1636–1646 (2016).
58. Tatsukawa, T. et al. Scn2a haploinsufficient mice display a spectrum of phenotypes affecting anxiety, sociability, memory flexibility and ampakine CX516 rescues their hyperactivity. *Mol. Autism* **10**, 15 (2019).
59. Lauterborn, J. C., Lynch, G., Vanderklish, P., Arai, A. & Gall, C. M. Positive modulation of AMPA receptors increases neurotrophin expression by hippocampal and cortical neurons. *J. Neurosci.***20**, 8–21 (2000).
60. Lauterborn, J. C. et al. Ampakines cause sustained increases in BDNF signaling at excitatory synapses without changes in AMPA receptor subunit expression. *Neuroscience* **159**, 283–295 (2009).
61. Jourdi, H. et al. Positive AMPA receptor modulation rapidly stimulates BDNF release and increases dendritic mRNA translation. *J. Neurosci.* **29**, 8688–8697 (2009).
62. Mackowiak, M., O'Neill, M. J., Hicks, C. A., Bleakman, D. & Skolnick, P. An AMPA receptor potentiator modulates hippocampal expression of BDNF: an in vivo study. *Neuropharmacology* **43**, 1–10 (2002).
63. Rex, C. S. et al. Restoration of long-term potentiation in middle-aged hippocampus after induction of brain-derived neurotrophic factor. *J. Neurophysiol.***96**, 677–685 (2006).
64. Woolley, M. L. et al. Evaluation of the pro-cognitive effects of the AMPA receptor positive modulator, 5-(1-piperidinylcarbonyl)-2,1,3-benzoxadiazole (CX691), in the rat. *Psychopharmacology***202**, 343–354 (2009).
65. Giralt, A. et al. The AMPA receptor positive allosteric modulator S 47445 rescues in vivo CA3-CA1 long-term potentiation and structural synaptic changes in old mice. *Neuropharmacology* **123**, 395–409 (2017).
66. Gad, S. C. et al. Tolerable levels of nonclinical vehicles and formulations used in studies by multiple routes in multiple species with notes on methods to improve utility. *Int. J. Toxicol.* **35**, 95–178 (2016).
67. Viscomi, M. T. et al. Methylprednisolone treatment delays remote cell death after focal brain lesion. *Neuroscience* **154**, 1267–1282 (2008).

Acknowledgements

L.B. and A.C. thank NYU Grossman School of Medicine and The Marlene and Paolo Fresco Institute for Parkinson's and Movement Disorders. The authors thank Dr. Giovanni Bellomo, University of Perugia, for discussion on α-synuclein protocol settings, Dr. Lorenzo Barolo and Dr. Francesco Mura, University of Rome La Sapienza, for allowing STEM acquisitions. This work was supported by grants from the Italian Ministry of University and Research PRIN 2022 grant 2022CAKAHL (CUP J53D23010930006, P.C., A.T.); the Italian Ministry of University and Research PRIN 2022 grant 2022XF7YYL_02 (A.U.); the Italian Ministry of University and Research PRIN 2022 Next Generation EU-PNRR-M4C2 grant P2022374Y9 (CUP J53D23016020001, A.T.); the Italian Ministry of Health, Ricerca Corrente 2024/2025 (A.C., P.C.); the research fellowship FISM (cod. 2023/BR/005, L.B.).

Author contributions

L.B. contributed to methodology, investigation, formal analysis, data curation, visualization, writing—original draft, and writing—review and editing. M.S. contributed to methodology, investigation, formal analysis, data curation, and writing—review and editing. A.M. contributed to methodology, investigation, and formal analysis. A.C. contributed to investigation, formal analysis, and visualization. J.C. contributed to investigation, formal analysis, writing—original draft, and writing—review and editing. M.D.C. and R.M. contributed to investigation, formal analysis, data curation, and visualization. C.C. and M.D.F. contributed to resources. A.U. contributed to data curation and writing—review and editing. M.T.V. contributed to conceptualization, methodology, investigation, formal analysis, data curation, visualization, supervision, writing—review and editing, and resources. P.C. contributed to conceptualization, methodology, supervision, writing—review and editing, and resources. A.T. contributed to conceptualization, methodology, formal analysis, data curation, visualization, supervision, writing—original draft, writing—review and editing, and resources.

Competing interests

The authors declare no competing interests.

Additional information

Supplementary information The online version contains supplementary material available at https://doi.org/10.1038/s41531-025-01075-z.

Correspondence and requests for materials should be addressed to Alessandro Tozzi.

Reprints and permissions information is available at http://www.nature.com/reprints

Publisher's note Springer Nature remains neutral with regard to jurisdictional claims in published maps and institutional affiliations.

Open Access This article is licensed under a Creative Commons Attribution-NonCommercial-NoDerivatives 4.0 International License, which permits any non-commercial use, sharing, distribution and reproduction in any medium or format, as long as you give appropriate credit to the original author(s) and the source, provide a link to the Creative Commons licence, and indicate if you modified the licensed material. You do not have permission under this licence to share adapted material derived from this article or parts of it. The images or other third party material in this article are included in the article's Creative Commons licence, unless indicated otherwise in a credit line to the material. If material is not included in the article's Creative Commons licence and your intended use is not permitted by statutory regulation or exceeds the permitted use, you will need to obtain permission directly from the copyright holder. To view a copy of this licence, visit http://creativecommons.org/licenses/by-nc-nd/4.0/.

© The Author(s) 2025

[1]Physiology and Biochemistry Section, Department of Medicine and Surgery, University of Perugia, Perugia, Italy. [2]Fondazione Malattie Rare Mauro Baschirotto BIRD Onlus, Longare (VI), Italy. [3]Neurology Section, Department of Medicine and Surgery, University of Perugia, Perugia, Italy. [4]Telematic University San Raffaele, IRCCS San Raffaele, Rome, Italy. [5]Neurology Section, Department of Neuroscience, Università Cattolica del Sacro Cuore, Rome, Italy. [6]Department of Neurosciences and Neurorehabilitation, IRCCS San Raffaele, Rome, Italy. [7]Department of Life Science and Public Health, Università Cattolica del Sacro Cuore, Rome, Italy. [8]Department of Environmental, Biological and Pharmaceutical Sciences and Technologies, University of Campania "L. Vanvitelli", Caserta, Italy. [9]CEINGE Biotecnologie Avanzate "Franco Salvatore", Naples, Italy. [10]Fondazione Policlinico Universitario Agostino Gemelli IRCCS, Rome, Italy. [11]Present address: Department of Life Science, Health and Health Professions, Link University, Rome, Italy. [12]These authors contributed equally: Laura Bellingacci, Miriam Sciaccaluga. [13]These authors jointly supervised this work: Paolo Calabresi, Alessandro Tozzi. ✉e-mail: alessandro.tozzi@unipg.it